

Search for gas accretion imprints in voids: II. The galaxy Ark 18 as a result of a dwarf-dwarf merger.

Evgeniya S. Egorova^{1*}, Oleg V. Egorov^{2,1†}, Alexei V. Moiseev^{3,1}, Anna S. Saburova^{1,4},
Kirill A. Grishin^{1,5}, Igor V. Chilingarian^{6,1}

¹ *Lomonosov Moscow State University, Sternberg Astronomical Institute, Universitetsky pr. 13, Moscow 119234, Russia*

² *Astronomisches Rechen-Institut, Zentrum für Astronomie der Universität Heidelberg, Mönchhofstr. 12–14, 69120 Heidelberg, Germany*

³ *Special Astrophysical Observatory, Russian Academy of Sciences, Nizhnii Arkhyz 369167, Russia*

⁴ *Institute of Astronomy, Russian Academy of Sciences, Pyatnitskaya st., 48, 119017 Moscow, Russia*

⁵ *Department of Physics, M.V. Lomonosov Moscow State University, 1 Vorobyovy Gory, Moscow, 119991, Russia*

⁶ *Center for Astrophysics – Harvard and Smithsonian, 60 Garden Street MS09, Cambridge, MA 02138, USA*

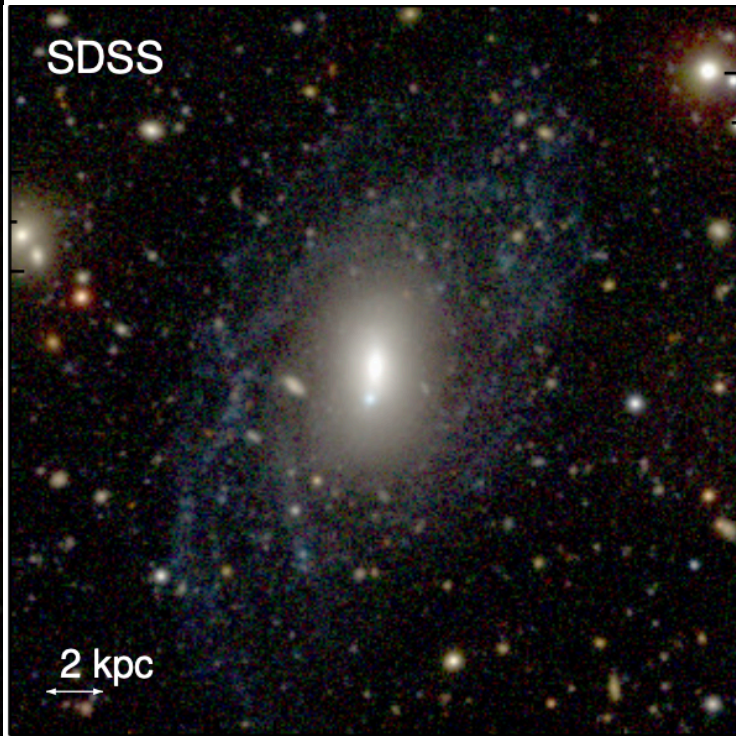
Accepted XXX. Received YYY; in original form ZZZ

ABSTRACT

The low-mass low-surface brightness (LSB) disc galaxy Arakelian 18 (Ark 18) resides in the Eridanus void and because of its isolation represents an ideal case to study the formation and evolution mechanisms of such a galaxy type. Its complex structure consists of an extended blue LSB disc and a bright central elliptically-shaped part hosting a massive off-centered star-forming clump. We present the in-depth study of Ark 18 based on observations with the SCORPIO-2 long-slit spectrograph and a scanning Fabry-Perot interferometer at the Russian 6-m telescope complemented by archival multi-wavelength images and SDSS spectra. Ark 18 appears to be a dark matter dominated gas-rich galaxy without a radial metallicity gradient. The observed velocity field of the ionised gas is well described by two circularly rotating components moderately inclined with respect to each other and a possible warp in the outer disc. We estimated the age of young stellar population in the galaxy centre to be ~ 140 Myr, while the brightest star-forming clump appears to be much younger. We conclude that the LSB disc is likely the result of a dwarf–dwarf merger with a stellar mass ratio of the components at least $\sim 5:1$ that occurred earlier than 300 Myr ago. The brightest star forming clump was likely formed later by accretion of a gas cloud.



Eridanus void
(Kniazev, Egorova, Pustilnik 2018)



Наблюдения: БТА ИФП+длинная щель

Центральная часть по параметрам
 близка к галактикам раннего типа, диск —
 к UGC и обычным LSB

- Возможные сценарии:
- Бар в LSB диске
 - Multispin system

Eridanus void (Kniazev, Egorova, Pustilnik 2018)

Table 1. Main properties and derived parameters of Ark 18. All values were obtained in this study unless otherwise noted

Parameter	Value
RA (J2000) ^a	00h51m59.62s
Dec (J2000) ^a	-00d29m12.2s
D ^a , Mpc	24.1
<i>m_B</i>	14.85
<i>M_B</i>	-17.2
SFR, M _⊙ yr ⁻¹	0.1
log <i>M_{HI}^b</i>	9.3
<i>M_{HI}</i> / <i>L_B</i>	2.3
<i>i</i> , deg	67 ± 1 (inner ^c) 58 ± 3 (outer ^d)
PA, deg	358 ± 3 (inner ^c) 344 ± 5 (outer ^d)
<i>V_{sys}</i> , km s ⁻¹	1627±9
12 + log (O/H)	8.20 ± 0.04

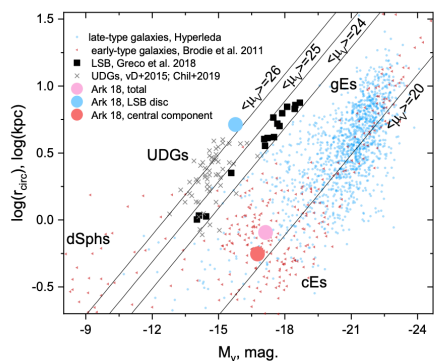
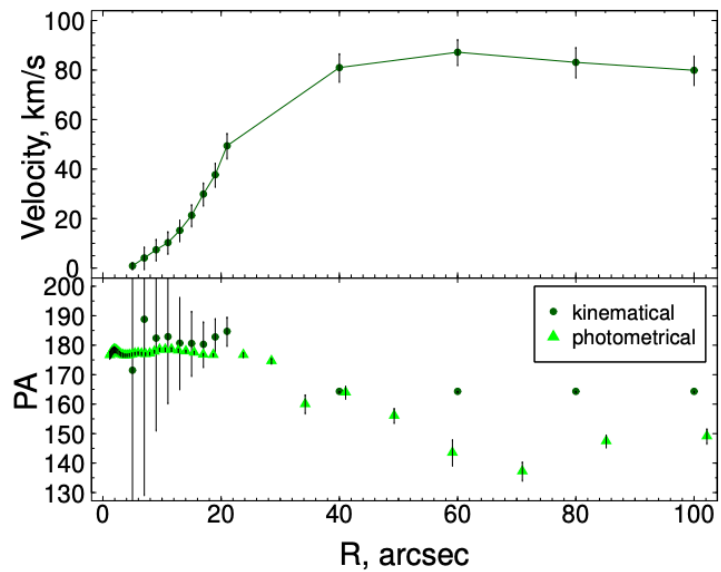
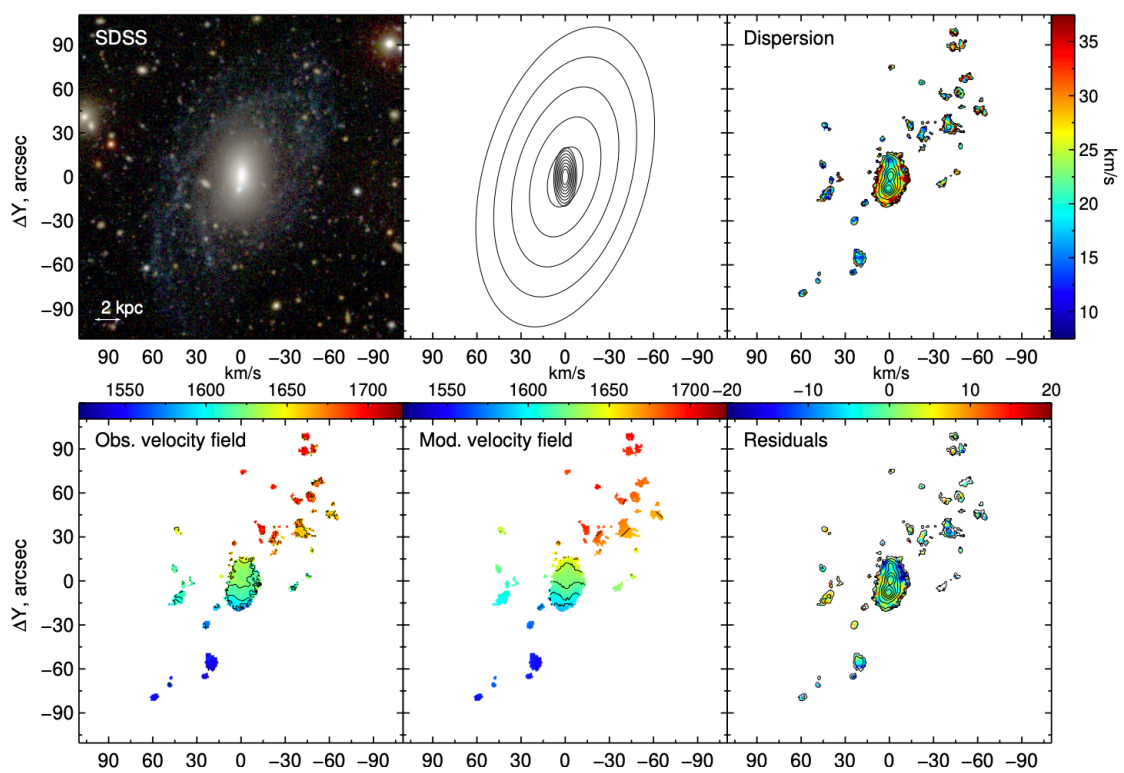
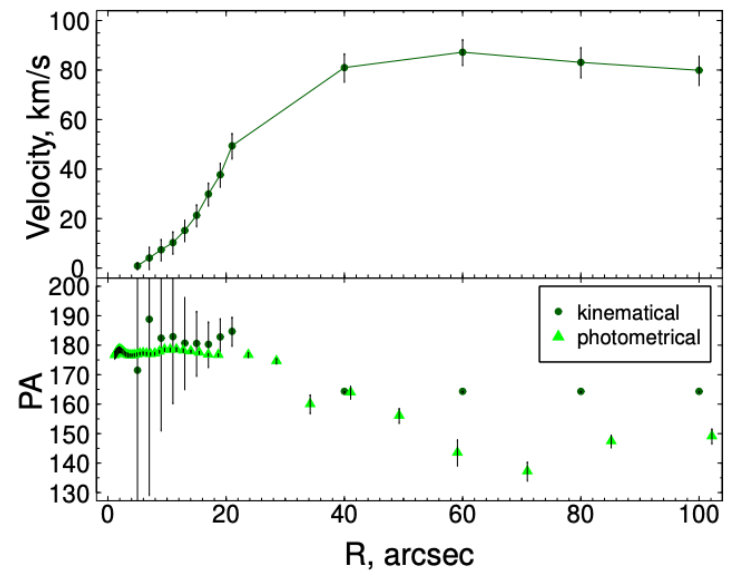
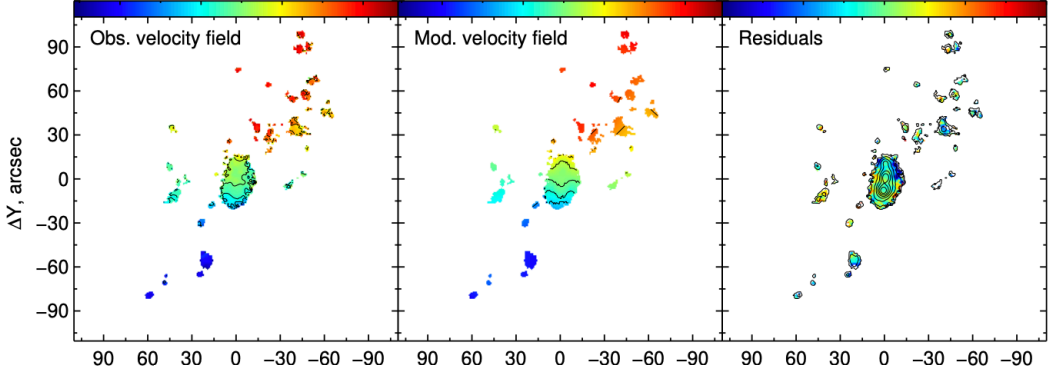
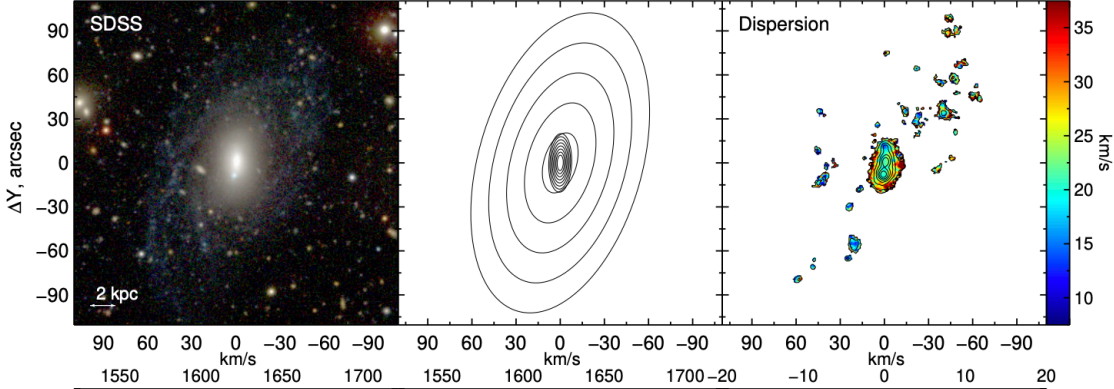


Figure 1. The position of Ark 18 in the size versus luminosity relation (big circles). On the y-axis we plot the logarithm of circularized effective radius estimated following Greco et al. (2018) $r_{circ} = (1 - \epsilon)^{1/2} r_{eff}$, where ϵ is ellipticity and r_{eff} is the radius containing the half of the luminosity. On the x-axis we give absolute V-band magnitude. Red, pink and blue circles are related to the central component, the overall galaxy and LSB disc. Black squares correspond to the position of LSB galaxies from Greco et al. (2018) for which the redshifts were available in Simbad database. Small red triangles demonstrate the position of early-type galaxies from Brodie et al. (2011). Small blue circles correspond to the late-type galaxies (with $t > 2$, where t is the morphological type) from the Hyperleda database. Grey crosses show the position of ultra diffuse galaxies from van



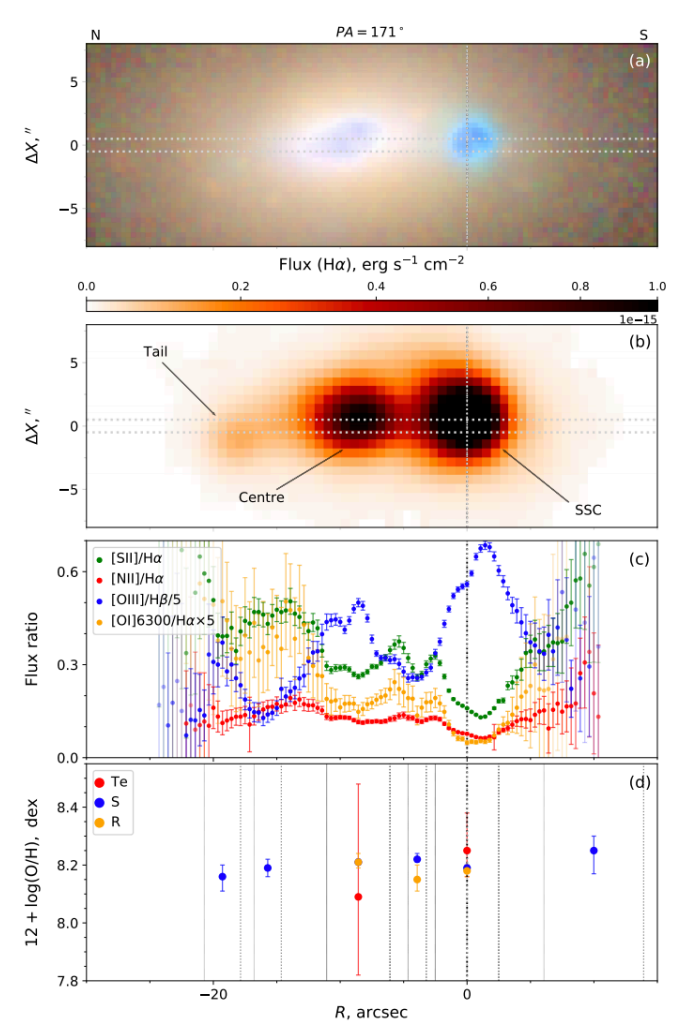
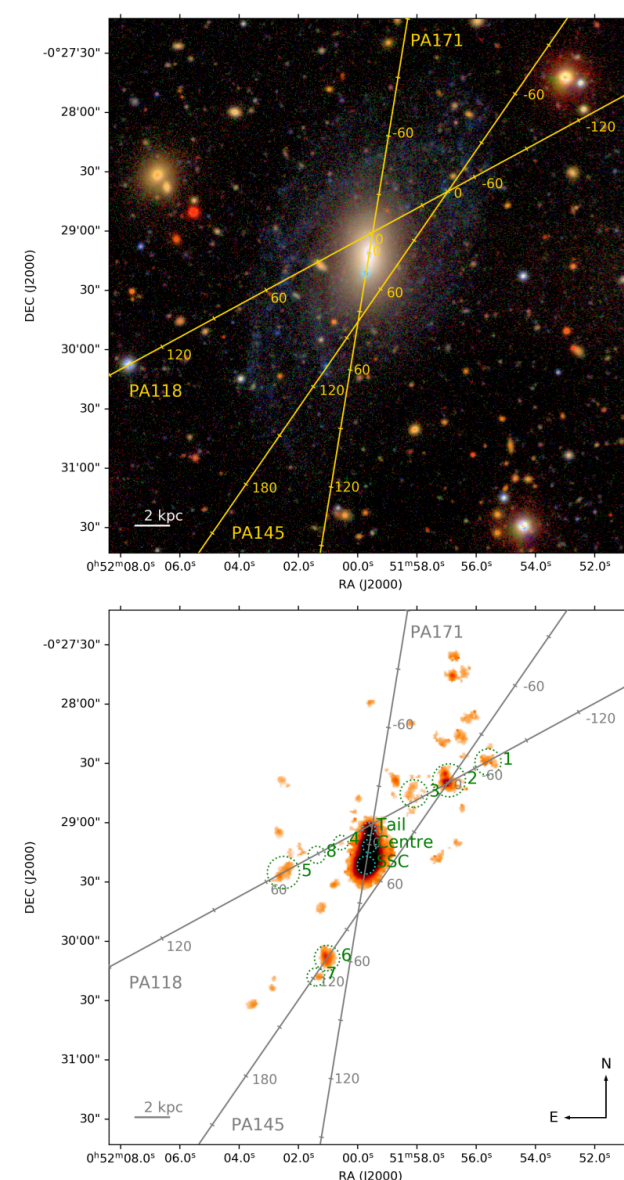
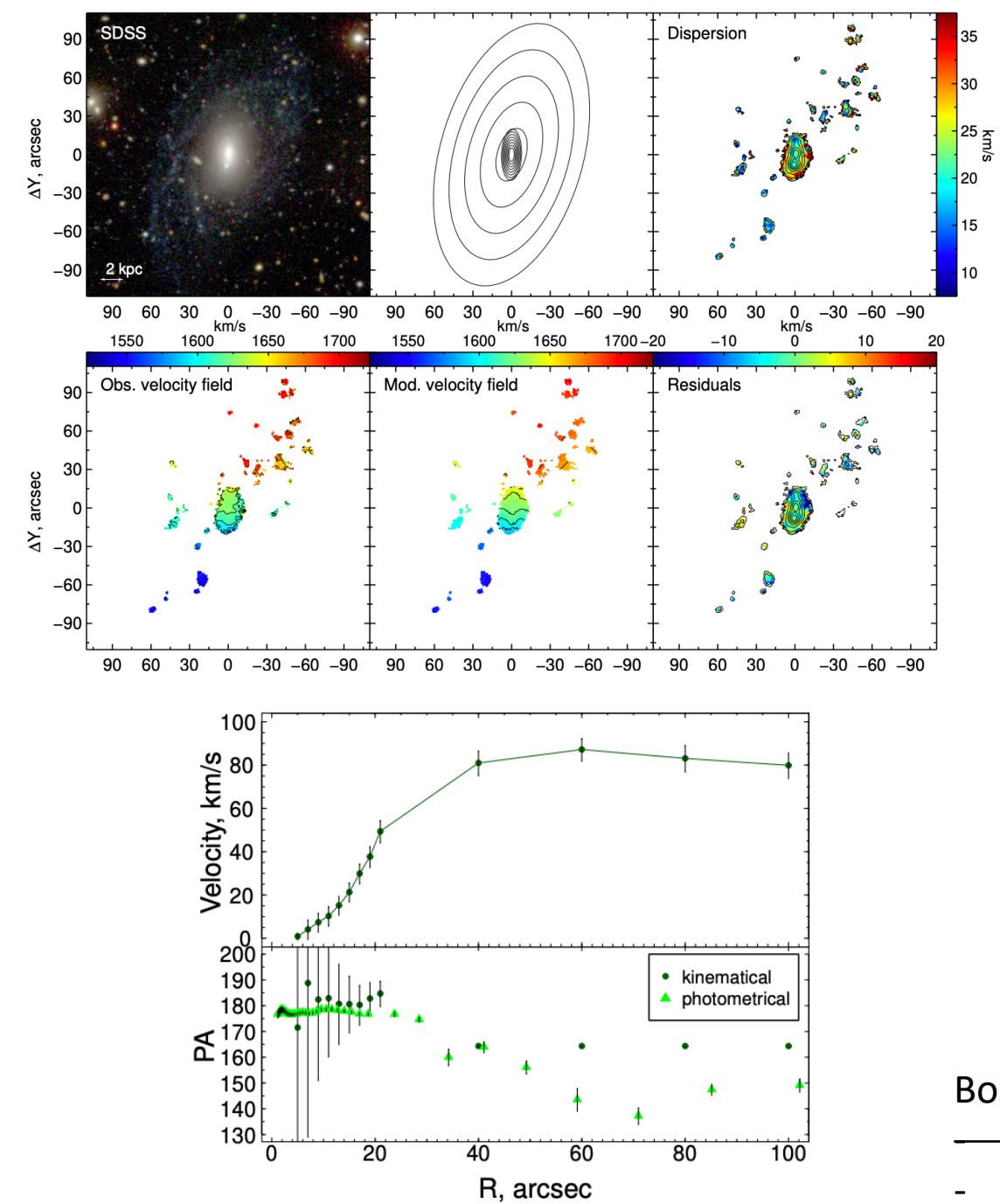
Возможные сценарии:

- Бар в LSB диске
- Multispin system



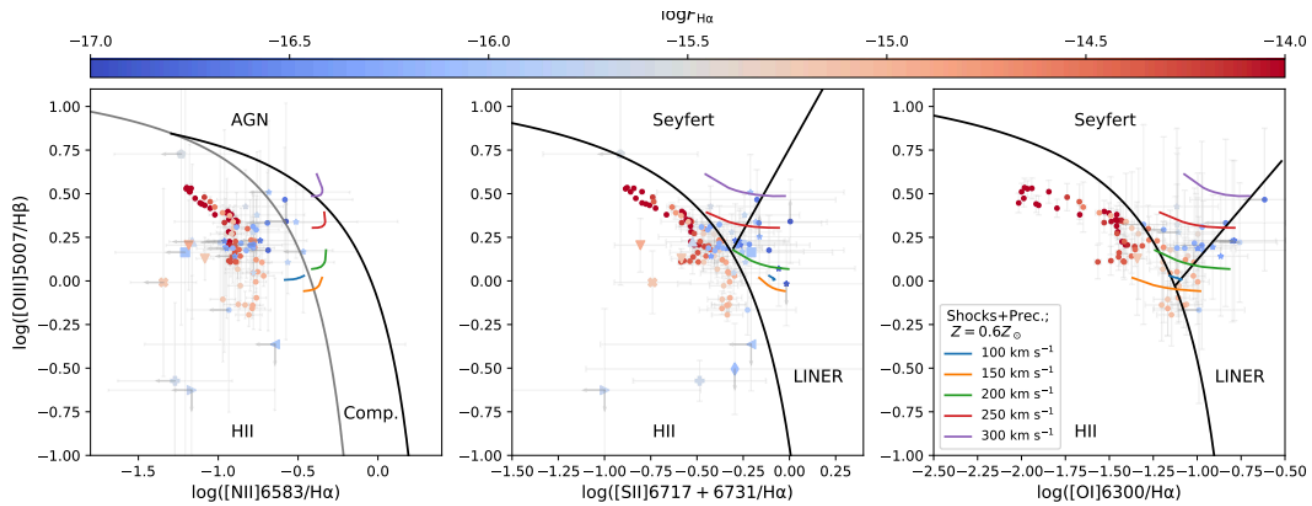
Возможные сценарии:
 — Бар в LSB диске
 - **Multispin system**

Аккреция из газовых филаментов?
 Падение спутников?



Возможные сценарии:
 — Бар в LSB диске
 - Multispin system

Figure 11. Results of the analysis of the emission-line spectrum obtained at PA=171. The position of the slit is overlaid on (a) SDSS *gri* colour image and (b) H α flux map by horizontal dotted lines. Panels (c) and (d) represent the distribution along the slit of the flux ratios and oxygen abundance, respectively. The oxygen abundance derived with three methods (T_e , S and R described in Section 3.5.2) are shown by different colours. The vertical lines on panel (d) show the limits of each region where the spectrum was integrated to estimate the oxygen abundance.



Почти все области – HII области, ионизованные массивными звездами. Вклад ударных волн может быть существенным на периферии центрального компонента. Подобное также наблюдается в галактиках с полярными кольцами (Egorov & Moiseev 2019).

Hence, from the decomposition of the $H\alpha$ line profiles we can draw a conclusion that the velocity dispersion of the ionised gas in the central regions of Ark 18 does not substantially differ from that in the rest of the galaxy, and the broadening of the $H\alpha$ line seen in Fig. 4 is caused by a broad underlying component. The latter could be explained by supernovae feedback from the brightest star-forming regions, while additional sources of shock waves may also cause supersonic motions at the outskirts of the central component.

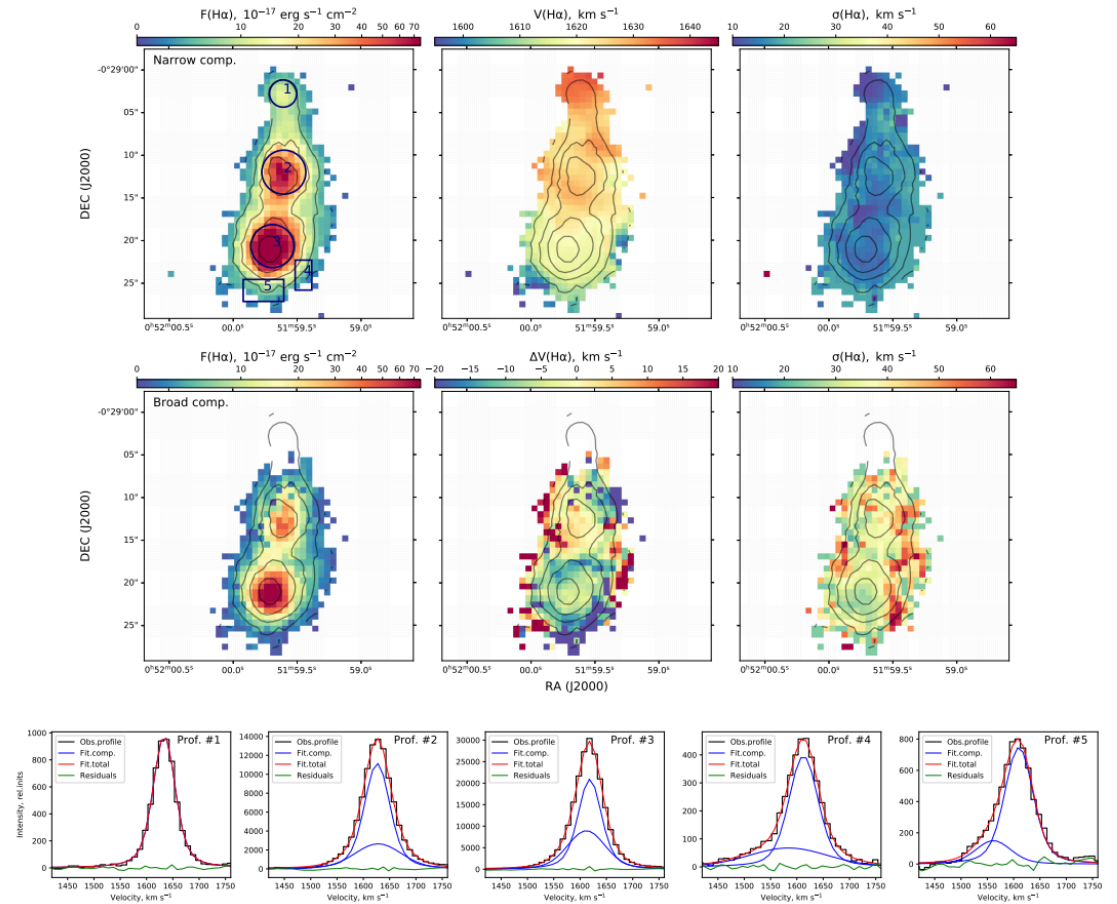


Figure 13. Decomposition of the $H\alpha$ data cube into narrow (top row) and broad (middle row) components for the central part of the galaxy. All pixels with $S/N < 15$ were masked. From left to right: the distribution of the $H\alpha$ flux, line-of-sight velocity (for the broad component its deviation $\Delta V(H\alpha)$ from that of narrow component) and velocity dispersion for corresponding component. The overlaid contours correspond to the distribution of $H\alpha$ flux for the narrow component. The bottom row demonstrates the examples of observed line profiles (black line) integrated over the regions shown in top-left panel, their decomposition onto individual components (blue line), resulting model (red line) and residuals (green line).

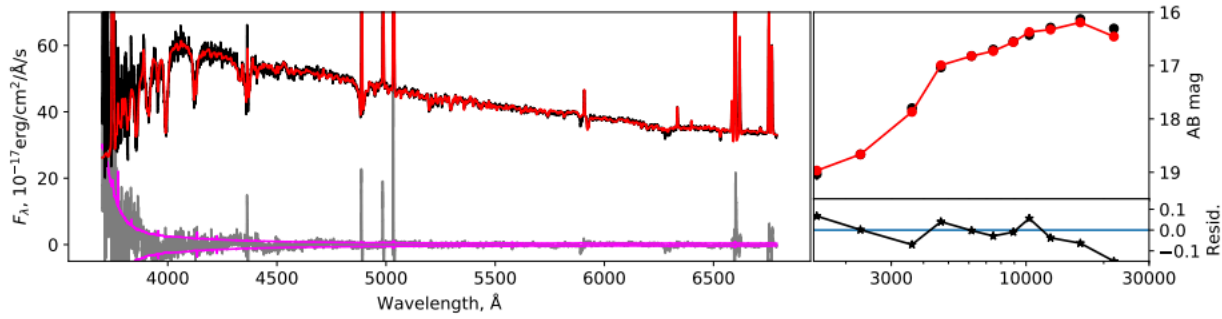


Figure 7. The SDSS spectrum for the “centre” region of Ark18 in F_λ units (left panel, black) and its SED in AB magnitudes (right panel, black), the best-fitting model spectra and SED (red), flux uncertainties (purple) and residuals (grey line and black asterisks). The SED fitting residuals are shown in the bottom-right panel.

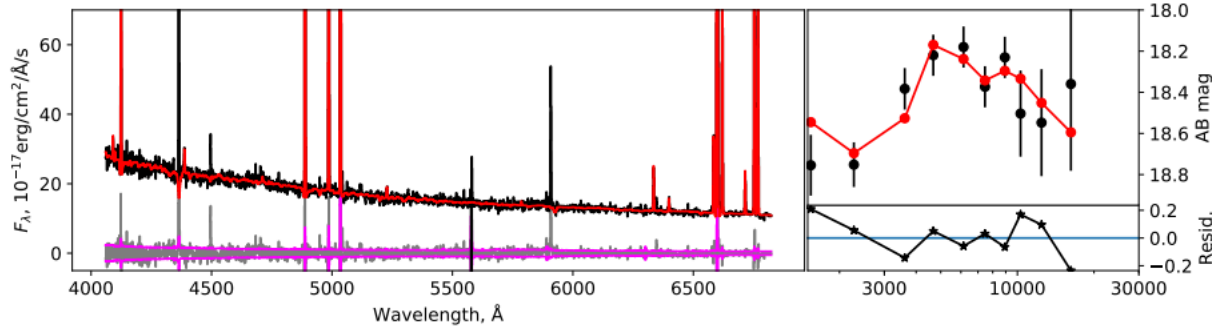


Figure 8. The SDSS spectrum for the “SSC” region of Ark18 in F_λ units and its best-fitting models. The symbols are the same as in Fig. 7

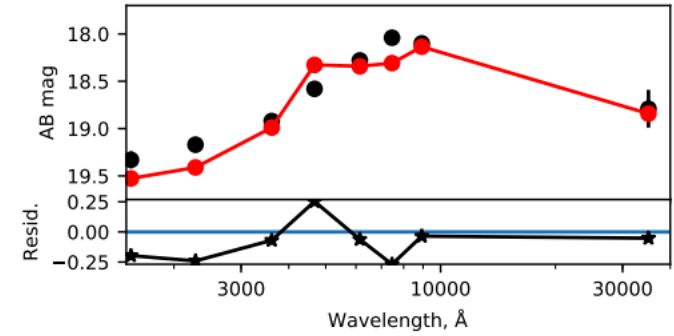


Figure 9. A broad-band SED (black circles) for the LSB disc of Ark 18 composed of broadband fluxes from far-UV (GALEX) to near-IR (Spitzer). The best-fitting model (red) is a SSP with the age of 127 Myr and metallicity fixed to -0.5 dex. The residuals are shown by black asterisks in the bottom panel.

- The central component demonstrates the continuous SF history during the large time with a probably constant SFR, and the young population that was formed recently (light-weighted age of the young stars in the “centre” is ~ 140 Myr, while the SSC appears to be much younger). We couldn’t obtain reliable estimate of the age of stellar population in LSB disc because of its faintness in UV and IR bands, however the observed SED is consistent with a presence of young stellar population with the age between 60 and 500 Myr.
- From the results of GALFIT modelling and spectral and SED fitting we have estimated the ratio of stellar masses of the central component and LSB disc to be at least $\sim 5 : 1$.

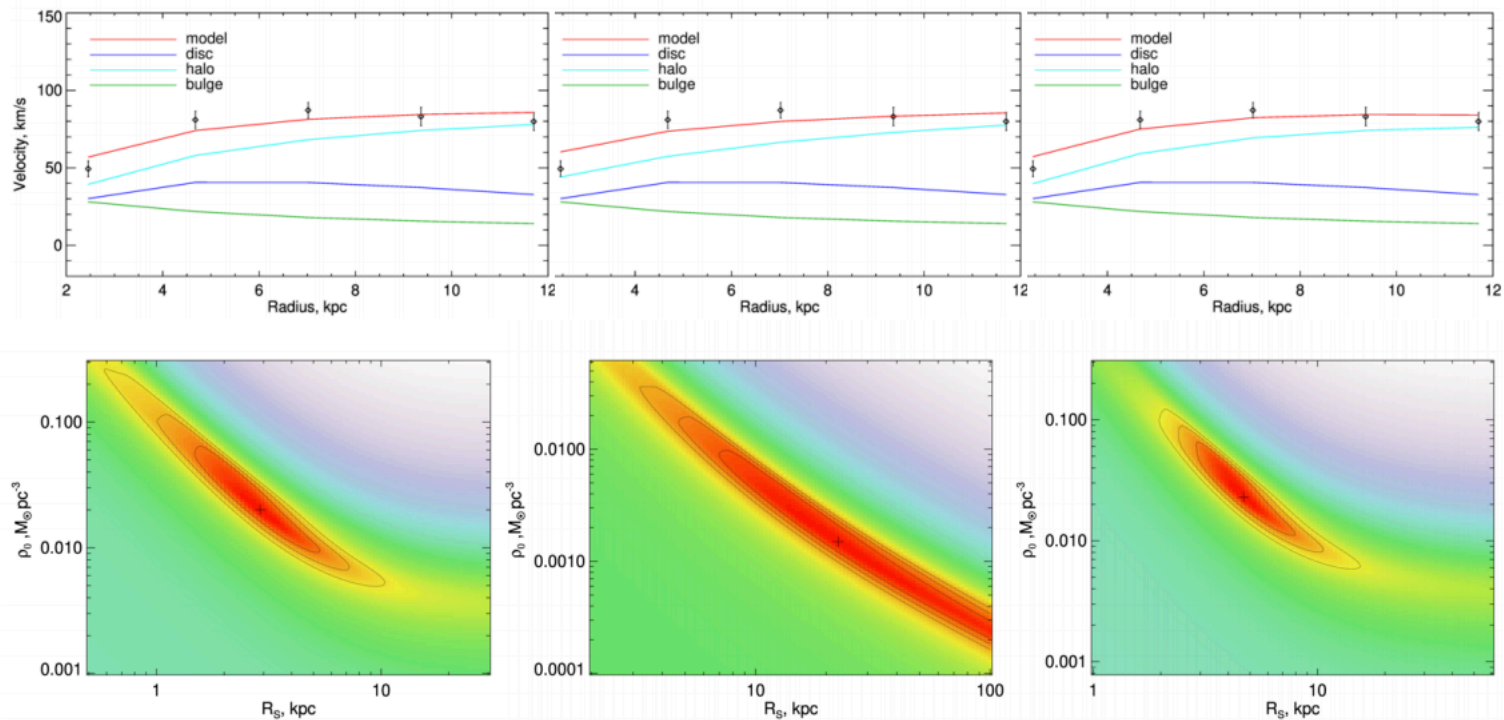


Figure 10. Top panel: the best-fitting models of the rotation curve of Ark 18 left — for the pISO profile of the DM halo, centre — for the NFW profile, right — to the Burkert profile. Bottom panel: χ^2 map for the parameters of dark halo, colour in the maps denotes the χ^2 value, the darker the color, the lower the χ^2 and the better is the fitting quality. The contours refer to 1σ , 2σ and 3σ confidence limits. The position of the parameters corresponding to the χ^2 minimum is shown by the cross in each map.

Table 3. The derived parameters of the dark halo with 1σ confidence limit errors. The columns contain the following data: (1) – dark halo profile; (2) and (3) – radial scale and central density of the DM halo; (3) – mass of DM halo inside of radius four disc radial scales 10.9 kpc

dark halo	R_s	ρ_0	M_{halo}
	kpc	$10^{-3} M_{\odot}/\text{pc}^3$	$10^{10} M_{\odot}$
Burkert	4.62 $^{+2.97}_{-1.56}$	22.86 $^{+40.44}_{-11.72}$	1.40 $^{+0.66}_{-0.28}$
NFW	22.28	1.51	1.47
pISO	2.84 $^{+2.02}_{-1.25}$	20.00 $^{+43.32}_{-10.55}$	1.46 $^{+0.63}_{-0.28}$

- Ark 18 is dark matter dominated gas-rich galaxy with dark halo having the radial scale and central density close to those observed in the “normal” high surface brightness discy galaxies with the same disc radii.

Галактика лежит на барионной зависимости TF.

Ubiquitous signs of interactions in early-type galaxies with prolate rotation

arXiv:2103.05006

Ivana Ebrov^{1*}, Michal Blek^{1,2}, Ana Vudragovic³, Mustafa K. Yildiz^{4,5}, and Pierre-Alain Duc²

¹ Nicolaus Copernicus Astronomical Center, Polish Academy of Sciences, Bartycka 18, 00-716 Warsaw, Poland

² Universite de Strasbourg, CNRS, Observatoire astronomique de Strasbourg (ObAS), UMR 7550, 67000 Strasbourg, France

³ Astronomical Observatory, Volgina 7, 11060 Belgrade, Serbia

⁴ Astronomy and Space Sciences Department, Science Faculty, Erciyes University, Kayseri, 38039 Turkey

⁵ Erciyes University, Astronomy and Space Sciences Observatory Applied and Research Center (UZAYBMER), 38039, Kayseri, Turkey

Received 17 February 2021; accepted 9 March 2021

ABSTRACT

Context. A small fraction of early-type galaxies (ETGs) show prolate rotation, i.e. they rotate around their long photometric axis. In simulations, certain configurations of galaxy mergers are known to produce this type of rotation.

Aims. We investigate the association of prolate rotation and signs of galaxy interactions among the observed galaxies.

Methods. We collected a sample of 19 nearby ETGs with distinct prolate rotation from the literature and inspected their ground-based deep optical images for interaction signs – 18 in archival images and one in a new image obtained with the Milankovic telescope.

Results. Tidal tails, shells, asymmetric/disturbed stellar halos, or on-going interactions are present in all the 19 prolate rotators. Comparing this with the frequency of tidal disturbance among the general sample of ETGs of a roughly similar mass range and surface-brightness limit, we estimate that the chance probability of such an observation is only 0.00087. We also found a significant overabundance of prolate rotators that are hosting multiple stellar shells. The visible tidal features imply a relatively recent galaxy interaction. That agrees with the Illustris large-scale cosmological hydrodynamical simulation, where prolate rotators are predominantly formed in major mergers during the last 6 Gyr. In the appendix, we present the properties of an additional galaxy, NGC 7052, a prolate rotator for which no deep images are available, but for which an HST image revealed the presence of a prominent shell, which had not been reported before.

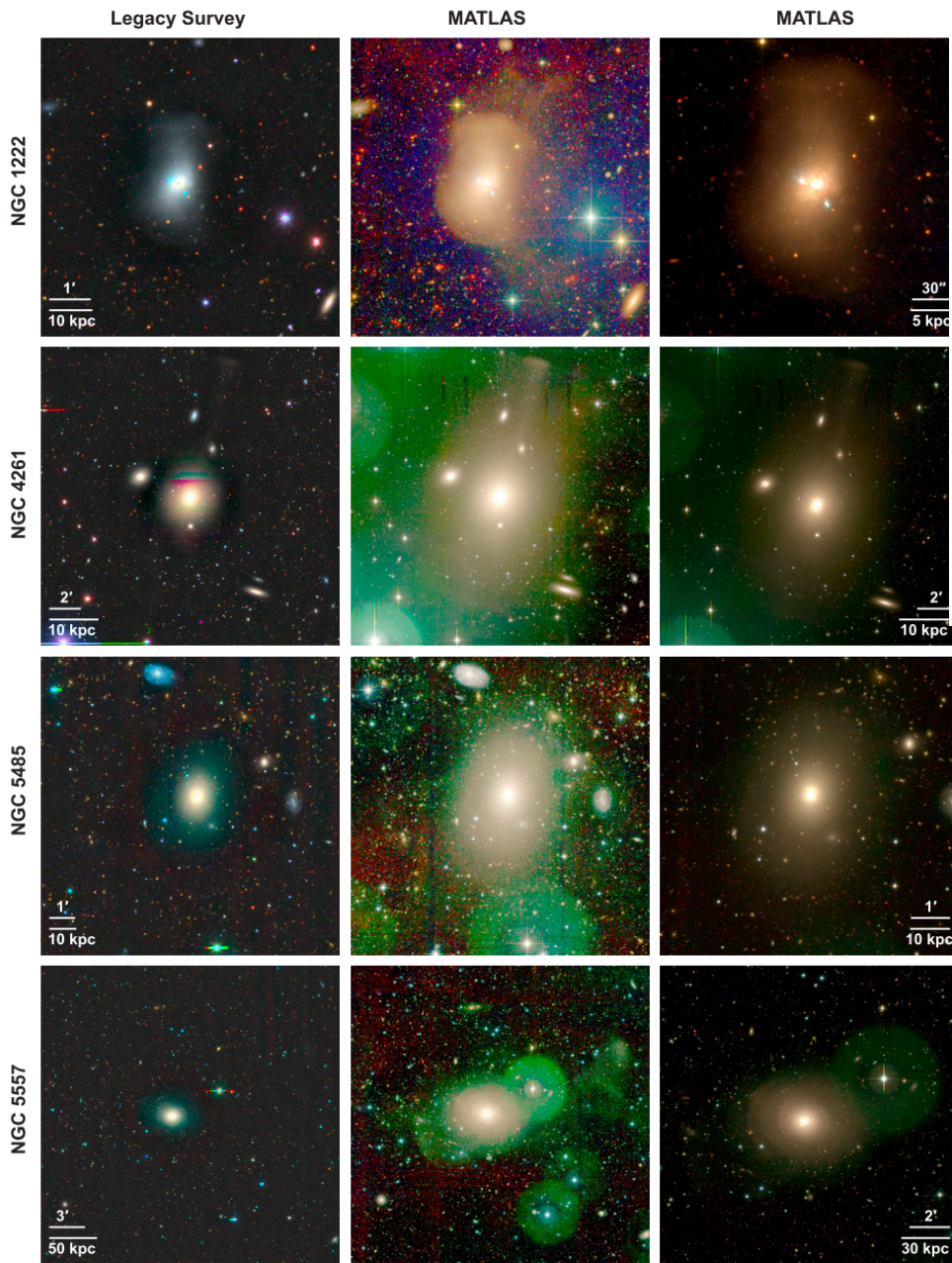


Fig. 3. Images of four prolate rotators from our sample. Left column: image extracted from the Legacy Surveys. Middle column: image from MATLAS showing the outer parts of the stellar halo with the same field of view as the image in the left column of the respective row. Right column: image from MATLAS showing more inner parts of the galaxy. North is up, east is to the left.



Fig. 7. Images of NGC 4874, one of the prolate rotators from our sample. Left: the SDSS image; middle: the Legacy Surveys image; right: the Legacy Surveys residual image. All panels have the same field of view. North is up, east is to the left.



Fig. 8. Images of NGC 7252, one of the prolate rotators from our sample. Left: Image taken by the Wide Field Imager on the MPG/ESO 2.2-metre telescope at ESO's La Silla Observatory in Chile with a total exposure time of more than four hours; Image credit: ESO. Right: HST/WFC3 image of the inner parts of the galaxy processed by Judy Schmidt to emphasize fine structures; Image credit: NASA & ESA, Acknowledgement: Judy Schmidt. North is up, east is to the left.

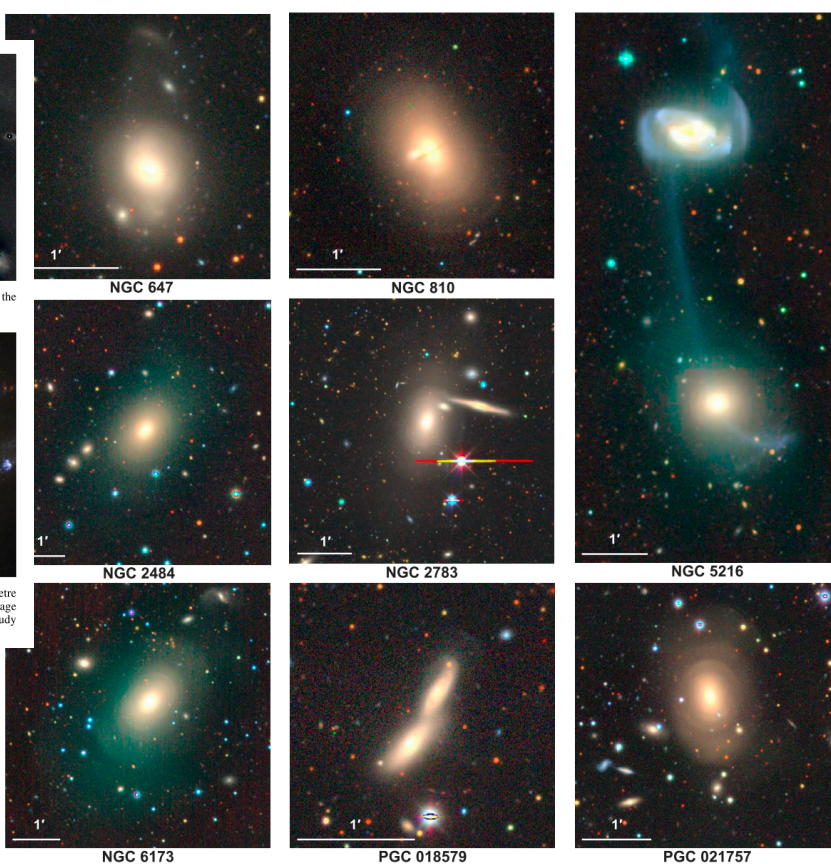


Fig. 1. Images of eight prolate rotators from our sample extracted from the Legacy Surveys. North is up, east is to the left.

19 ETG с prolate rotation – ATLAS3D, CALIFA, and the literature.

Проверяли, есть ли признаки взаимодействия, и во всех случаях нашли их.

Согласуется с результатами Illustris, где prolate rotation получается в основном в результате больших слияний в течение последних бмлрд.лет.

We compared this with the tidal disturbance frequency among the galaxies with a similar mass range drawn from the MATLAS sample – a volume-limited general sample of nearby ETGs. We verified that the MATLAS survey has a similar or better surface-brightness limit than the images of the prolate rotators. We found that the chance probability of observing 19 out of 19 ETGs with interaction signs is only 0.00087.